

Steady-State Visually Evoked Potentials Elicited by Multifrequency Pattern-Reversal Stimulation

Bettina Hohberger¹, Jan Kremers¹, and Folkert K. Horn¹

¹ Department of Ophthalmology and Eye Hospital, University Hospital Erlangen, Germany

Correspondence: Folkert K. Horn, Department of Ophthalmology and Eye Hospital, Friedrich-Alexander-University Erlangen-Nürnberg, D-91054 Erlangen, Schwabachanlage 6, Germany. e-mail: folkert.horn@uk-erlangen.de

Received: 26 July 2018

Accepted: 17 December 2018

Published: 28 February 2019

Keywords: steady-state; multifocal VEP; pattern reversal; objective visual field test; signal-to-noise ratio

Citation: Hohberger B, Kremers J, Horn FK. Steady-state visually evoked potentials elicited by multifrequency pattern-reversal stimulation. *Trans Vis Sci Tech.* 2019;8(1):24. <https://doi.org/10.1167/tvst.8.1.24> Copyright 2019 The Authors

Purpose: It has been shown that multifrequency stimulation with multifocal electroretinography can reduce recording time without a loss in signal-to-noise ratio. Here, we studied the applicability of multifrequency stimulations for steady-state visually evoked potential (VEP) recordings.

Methods: Multifrequency VEPs were recorded monocularly from 10 healthy subjects using pattern-reversal stimuli. The reversal frequency varied between 5 and 30 Hz. Pattern-reversal checkerboard stimuli were generated using four square arrays, each containing 100 light-emitting diodes (LEDs), positioned in four quadrants. Each array had a temporal frequency that differed slightly from the nominal frequency. The long duration of the data acquisition ensured that the slightly different stimulus frequencies in the four LED arrays can be resolved and that the responses to the stimulus in each array can be distinguished (e.g., with a frequency resolution: 0.011 Hz at 12 Hz). The best response from the four recording electrode configuration, defined as the recording with the maximal signal-to-noise ratio, was used for further analysis. Algorithmic latencies were calculated from the ratio of phase data and frequencies in a range of 4 and 20 Hz.

Results: Quadrant-VEPs with simultaneous pattern-reversal stimulation yielded a significant dependency on temporal frequency and stimulus location. The frequency range leading to the maximal response amplitude was between 10 and 12 Hz. Response phases decreased approximately linearly, with increasing temporal frequency suggesting a mean algorithmic latency between 112 and 126 ms.

Conclusions: Multifrequency stimulation using LED arrays is an efficient method for recording pattern-reversal VEPs while all stimuli are presented at the same time.

Translational Relevance: Simultaneously recorded VEPs as performed by the multifrequency method can be used for objective measurements of visual field defects.

Introduction

Visually evoked potentials (VEPs) are electroencephalographic potentials that are elicited by visual stimulation and therefore may offer information about the integrity of the cortical visual pathways and their subcortical inputs. Furthermore, VEPs are a potential tool to investigate pathways with importance for visual perception.

VEPs elicited by repetitive stimuli at relatively high temporal frequencies result in so-called steady-state responses that can be characterized by a limited number of discrete frequency components after Fourier transform.¹ Responses at other frequencies, caused by noise or artifacts (e.g., eye movements,

myographic noise, alpha waves^{2,3}), can be separated from the signal and will not disturb further analysis. In contrast to applying m-sequences for multifocal steady-state stimulation, as was done previously,⁴ we here used a multifrequency method. It has been shown that fundamental and higher harmonic components in the frequency domain have extremely small bandwidths and can be very stable.^{5,6} As a consequence, if stimuli with only slight differences in temporal frequency are delivered simultaneously, the responses elicited by these stimuli can be separately analyzed in the frequency domain (i.e., after Fourier transform), provided that the time of a measurement is sufficiently long to resolve the temporal frequency differences. This method may enable efficient simul-

taneous recordings of steady-state responses to spatially discrete stimuli and is therefore called multifrequency stimulation. If the frequency differences are small enough to ensure that identical mechanisms and pathways underlie the measured responses, then the differences in response properties can be fully attributed to the spatial position of the different stimuli. One assumption is that there are no nonlinear interactions between the stimuli that might introduce frequencies that are not present in the stimuli. Regan and colleagues were the first, to our knowledge, to use multifrequency stimulation for VEP recordings.⁷ Using a semiautomatic multichannel Fourier analyzer, the VEPs were analyzed.

The advancement of light-emitting diode (LED) light sources for stimulation enabled an easy and cost-efficient use of multifrequency stimulation with high temporal resolution and thus with only minor differences in temporal frequencies. This stimulation has been shown to improve the signal-to-noise ratio (SNR) in multifocal electroretinography (ERG) recordings and/or to decrease the recording time⁸ in comparison to conventional m-sequence stimulation.⁹ The SNR is probably increased because of the continuous stimulus presentation (unlike in the m-sequence paradigm, where stimulus presentation is continuously interrupted). Thus, the fast Fourier transformation (FFT) is conducted on the whole recording, with no need for a separate time window for calculation of the noise.¹⁰

The multifrequency stimulation may have similar advantages for VEP recordings and their analysis. The aim of the present study was to investigate the temporal frequency resolution for extrafoveal stimulation by pattern-reversal VEP recording in healthy subjects using optimized electrode positions and LED stimulation. We further studied the dependency of response amplitude and phase on temporal frequency.

Methods

Experimental Design and Stimulus

Stimulation and recording of the VEPs were performed with a modified RETIScan system (Roland Consult, Brandenburg, Germany). Pattern-reversal stimuli were generated by LED arrays consisting of 100 white LEDs per array (TLMW3100; Vishay Semiconductors, Malvern, PA) arranged in a checkerboard-like manner. The method and results for different pattern-reversal frequencies with central stimulation have been given earlier.¹¹ Each half of

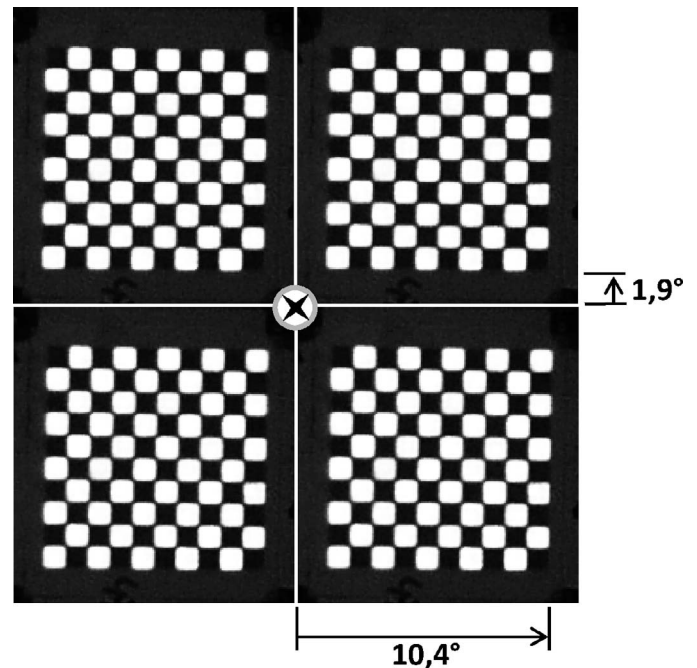


Figure 1. Stimulus arrangement of four LED arrays.

the checkerboard pattern in an array was formed by a set of 50 LEDs with a common power supply that was adjusted to equal luminance of the LEDs using a digital photometer (Tektronix J16/J6503; Tektronix Inc., Beaverton, OR). A single electrical pulse at the trigger input of each array caused a counterphase switch between the first and second sets of the LEDs.

A matrix of light-tight material (thickness: 0.5 mm) was mounted between the LEDs to block light from neighboring LEDs and to achieve a contrast of nearly 100%. This spatial arrangement ensured that each LED provided the luminance in a 4×4 -mm rectangular field. One LED array stimulated a retinal area of 8.5° . The spatial frequency was 0.58 cyc/deg at the viewing distance of 30 cm. Each array was covered by thin rice paper that acted as diffusor of the light from each LED. Four LED arrays were mounted on a plate for quadrant stimulation. The margin between two neighboring LED fields was 3.8° (see Fig. 1 for a sketch of the stimulus arrangement). A fixation LED was positioned centrally between the arrays so that each array stimulated a distinct quadrant. The measurements were made with natural pupils and appropriate correction for distance and presbyopia. The LEDs in each array were either switched on or off, resulting in a reversing checkerboard pattern. The mean luminance of the checkerboard field was 170 cd/m^2 (and thus modulated between 0 and 340 cd/m^2). The recordings were performed in a darkened room.

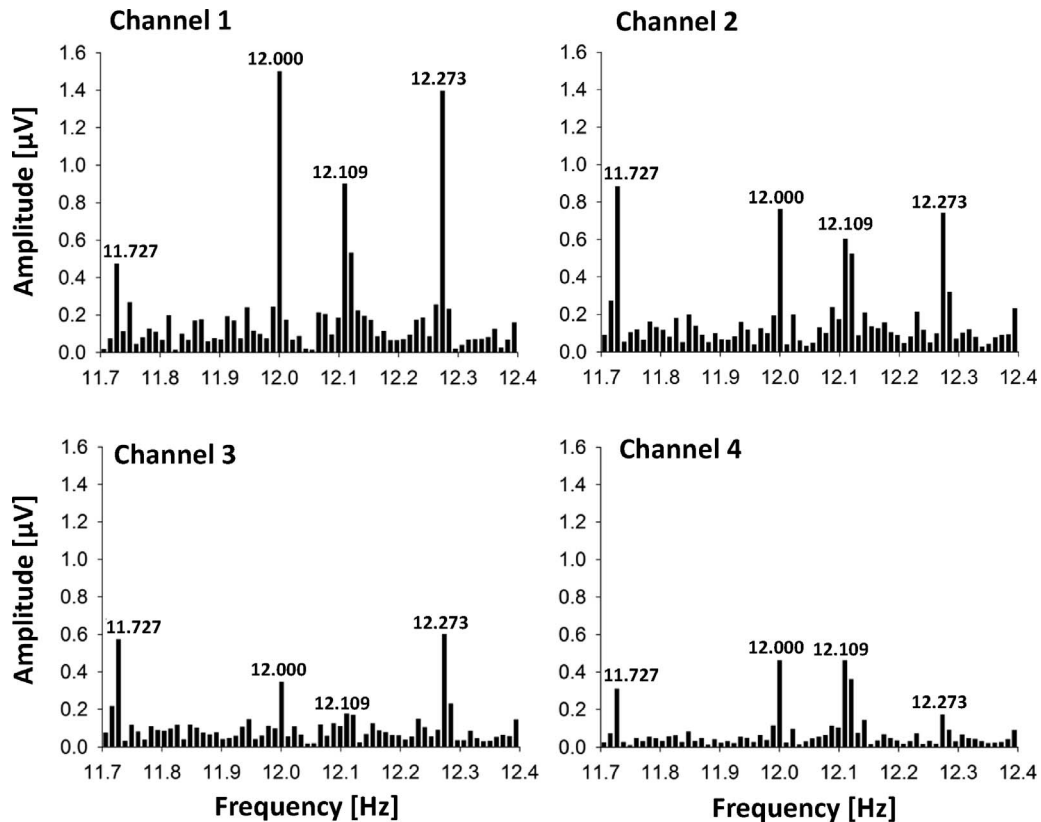


Figure 2. Spectra of steady-state VEP obtained from the four recording channels for a nominal 12-Hz pattern-reversal frequency. The measurement time was 91.5 seconds. In this time span, the number of reversals at each LED array was 1073, 1098, 1108, and 1123, respectively. Thus, the exact frequency of each LED array was 11.727 (left upper), 12.000 (right upper), 12.109 (left lower), and 12.273 Hz (right lower). For the most part, the stimulus frequencies were detected in all recording channels. The spectra deliver nine or more nonstimulus frequencies between the stimulus frequencies, which can be used to calculate the SNR.

The checkerboard pattern-reversal frequencies varied between 5 and 30 Hz (equivalent to base frequencies between 2.5 and 15 Hz). Here, only pattern-reversal frequencies are used.

The responses to 11 different nominal temporal frequencies (5, 6, 8, 10, 12, 14, 16, 18, 20, 25, 30 Hz) of the LED stimuli were measured. To achieve multifrequency stimulation, the pattern-reversal frequency in the four LED arrays differed slightly. For example, at the nominal frequency of 12 Hz, the exact temporal frequencies in the four arrays were 11.727 Hz (upper-left LED array), 12.000 Hz (upper right), 12.109 Hz (lower left), and 12.273 Hz (lower right). The total measuring time at each frequency was chosen to contain integer numbers of periods for all four stimuli. Thus, the total measuring time varied between 38.93 seconds (at 30 Hz nominal frequency) and 213.8 seconds (at 5 Hz nominal frequency), and the frequency resolution was between 25.69 mHz (30 Hz) and 4.677 mHz (5 Hz). The number of reversals

per measurement varied between 1044 (at 4.883 Hz) and 1193 (at 30.642 Hz).

The differences between stimulus frequencies were sufficiently small to ensure that identical physiological mechanisms were activated by the four LED arrays. Sampling frequency and sample time were sufficient to ensure a high temporal resolution of the FFT and to distinguish between the responses to the different stimulus frequencies. For example, the 12.000 Hz stimulation used 1098 reversals in 91.5 seconds and a sample frequency of 804 Hz, resulting in a frequency resolution of 10.9 mHz and 67 samples for one cycle. Figure 2 displays the amplitudes of the frequency components of a VEP recording in one subject (four different channels were used, see below) to a 12-Hz stimulus. Only the frequency components close to the stimulus frequency are displayed. Clearly, the exact stimulus frequencies (11.727, 12.000 Hz, 12.109 and 12.273 Hz, see above) can be distinguished.

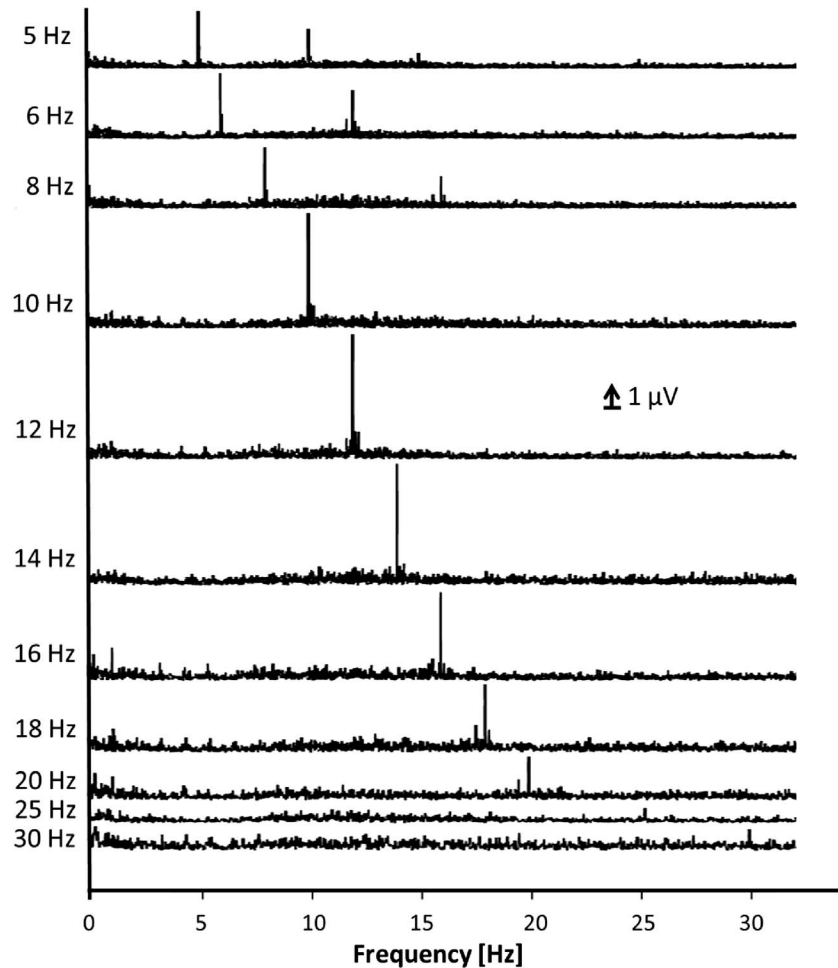


Figure 3. Spectra obtained from a recording at one channel (electrodes above and below inion) for all frequencies tested.

VEP Recordings

Pattern-reversal VEPs were recorded with four different electrodes placed on the subject's skull using an electrode fixation cap (Easycap GmbH, Herrsching am Ammersee, Germany) with positions of the electrodes as suggested by Klistorner and Graham¹² for the multifocal VEP (A: 2.5 cm above; B: 4 cm left; C: 4 cm right; and D: 4.5 cm below the inion). Due to the flexible characteristic of the fixation cap, the distances between the electrodes were adjusted to differences in the subjects' head sizes. In the past, several electrode configurations have been studied for peripheral VEP recordings, and it has been shown that multichannel VEP recordings outmatch recording systems using only one channel.^{12,13}

Recordings from four different channels (i.e., electrode pairs) were evaluated (channel 1: A–D; channel 2: B–C; channel 3: B–D; channel 4: C–D). An additional ground electrode was placed on the

forehead. The electrodes were filled with electrode paste (GE Medical Systems Information Technologies, Freiburg, Germany). The skin was prepared with skin preparation gel (Nuprep; Weaver and Company, Aurora, CO). The impedances between the electrodes were less than 5 kOhm. Biosignals were band-passed filtered with 1- and 100-Hz cut off frequencies and digitized with the appropriate sampling frequency (see above). All measurements were repeated in a separate session, and the results were subsequently averaged in the frequency domain.

Analysis

The signals were analyzed off-line with self-written signal-processing software. The amplitudes at the pattern-reversal frequencies were extracted using FFT. Figure 3 shows spectra of recordings at channel 1 for all stimulus frequencies (5–30 Hz). At reversal frequencies of 8 Hz and lower, higher harmonics were observed. In the present study, only the fundamental

components were considered. From the four channels (electrode configurations), the recording with maximal SNR at the stimulus frequency was chosen for further analysis (“best of” analysis for the amplitudes). The SNR was defined as the amplitude of the signal at stimulus frequency divided by the amplitudes at both next but one neighboring frequencies (at which no response was elicited by the stimulus).¹⁴ To judge possible differences between measurements, mean values and 95% confidence intervals (CI) are shown for amplitudes and SNR.

Phase data for each channel and LED array were plotted as a function of the stimulation frequency for all responses at the first and second test. Phase data of responses with SNR smaller than 2 dB were excluded from further phase analyses. This SNR criterion ensures that 75% of the data were included in the subsequent phase analyses. The phases depended in an approximately linear manner on temporal frequency (see Results). The slopes of the regression lines were used to calculate the algorithmic latencies using the formula $L = -[(\Delta\text{phase}/\Delta F) \times 1000 \text{ ms}/360^\circ]$, where L is the algorithmic latency and F is temporal frequency.

Subjects

The study included 10 randomly selected eyes of 10 normal subjects (seven females and three males, mean age 45.3 ± 19 years) without miotic or mydriatic eye drops and with their normal corrections. Informed consent, including agreement for data collection, was obtained from each participant. The registered study (available in the public domain at www.clinicaltrials.gov, NCT00494923) followed the tenets of the Declaration of Helsinki for research involving human subjects and was approved by the local ethics committee.

Results

Comparison of First and Second VEP Recordings

The reliability of the VEP recordings was studied for all 11 stimulus frequencies (5–30 Hz) with a retest of the measurements in a different session. Figure 4a displays a Bland-Altman plot of the data in which the amplitude difference between the first and second measurement is given as a function of their average. At very small amplitudes, the differences between the first and second measurements were also small. The

maximal amplitude differences were about $1 \mu\text{V}$, and there was no systematic dependency (Spearman rank test) of the difference on the mean amplitude. The reliability analysis (Fig. 4b.) reveals significant correlation between the first and second measurement at all LED arrays for frequencies between 10 and 14 Hz.

Frequency Transfer of the VEP Responses

Amplitudes

Figures 5a and 5b show the maximal SNRs and the corresponding response amplitudes (means \pm 95% CI) as a function of the stimulus frequency plotted separately for the four LED arrays in 10 normal subjects. Logarithmic transformation was performed to achieve a normal distribution of the data. The response amplitudes were maximal at a frequency between 10 and 12 Hz, although the SNR can be maximal at other frequencies. The multifocal VEP amplitudes of the right upper quadrant were slightly larger than the amplitudes of the other three quadrants for all frequencies. This difference was significant (Wilcoxon test with consideration of the Bonferroni correction), with exception of 8-Hz stimulation. At 10 Hz, nominal frequency the mean amplitudes were $0.41 \mu\text{V}$ (upper left), $0.48 \mu\text{V}$ (lower left), $0.82 \mu\text{V}$ (upper right), and $0.75 \mu\text{V}$ (lower right). Reliable responses at high stimulus frequencies above 20 Hz could be measured only at the upper-right LED array. The amplitudes at were not at stimulus frequencies (mean noise level: $0.11 \pm 0.06 \mu\text{V}$) showed highest values at frequencies where alpha components can be expected (around 10 Hz). A statistical comparison of the noise at all frequencies reveals no significant difference between the four quadrants (Friedman test).

Phases

Figure 6a displays the phases from three subjects for the first and second measurements as a function of stimulus frequency separately for the four electrode positions. As the FFT gives phases in modulo of 360° between -180 and $+180$, integer multiples of 360° were added or subtracted to obtain the estimated phases. We assumed that the phase decreases monotonously with increasing frequencies. For these plots, we assumed that the phases at low frequencies were less than 360° apart for the different subject and different LED arrays. Although the phase range was relatively large, the data indicate that the phases depend linearly on frequencies, indicating that they are mainly caused by the latency between stimulus and response. The

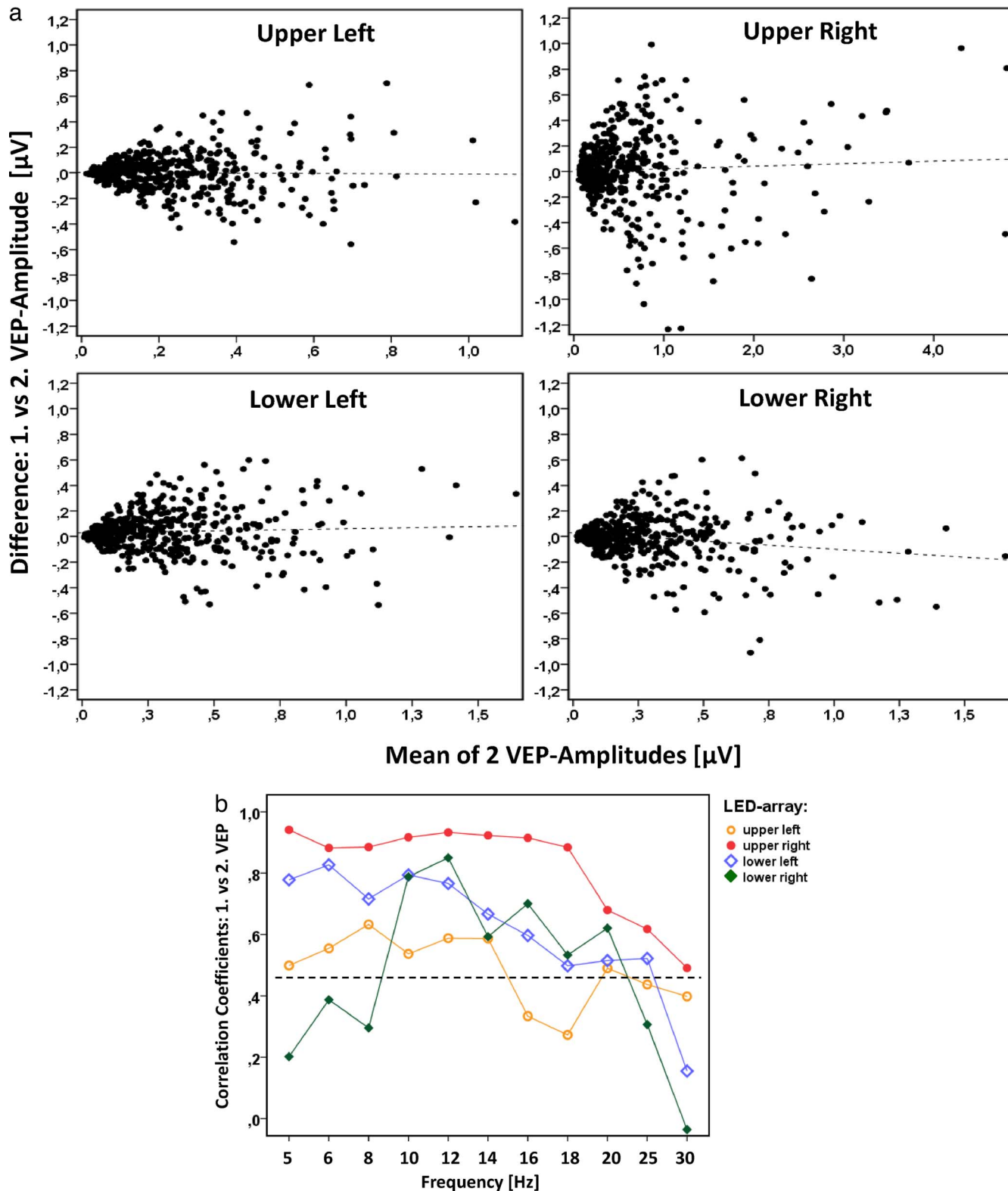


Figure 4. Reliability of multifocal VEPs: (a) Bland-Altman analyses of all first and second VEP amplitudes reveal the variation between measurements in four quadrants. There was no significant relationship between difference and mean of the amplitudes. (b) Correlation coefficients of the reliability analysis for first and second measurement at four LED arrays. The *dotted line* indicates the significance level (with consideration of Bonferroni correction).

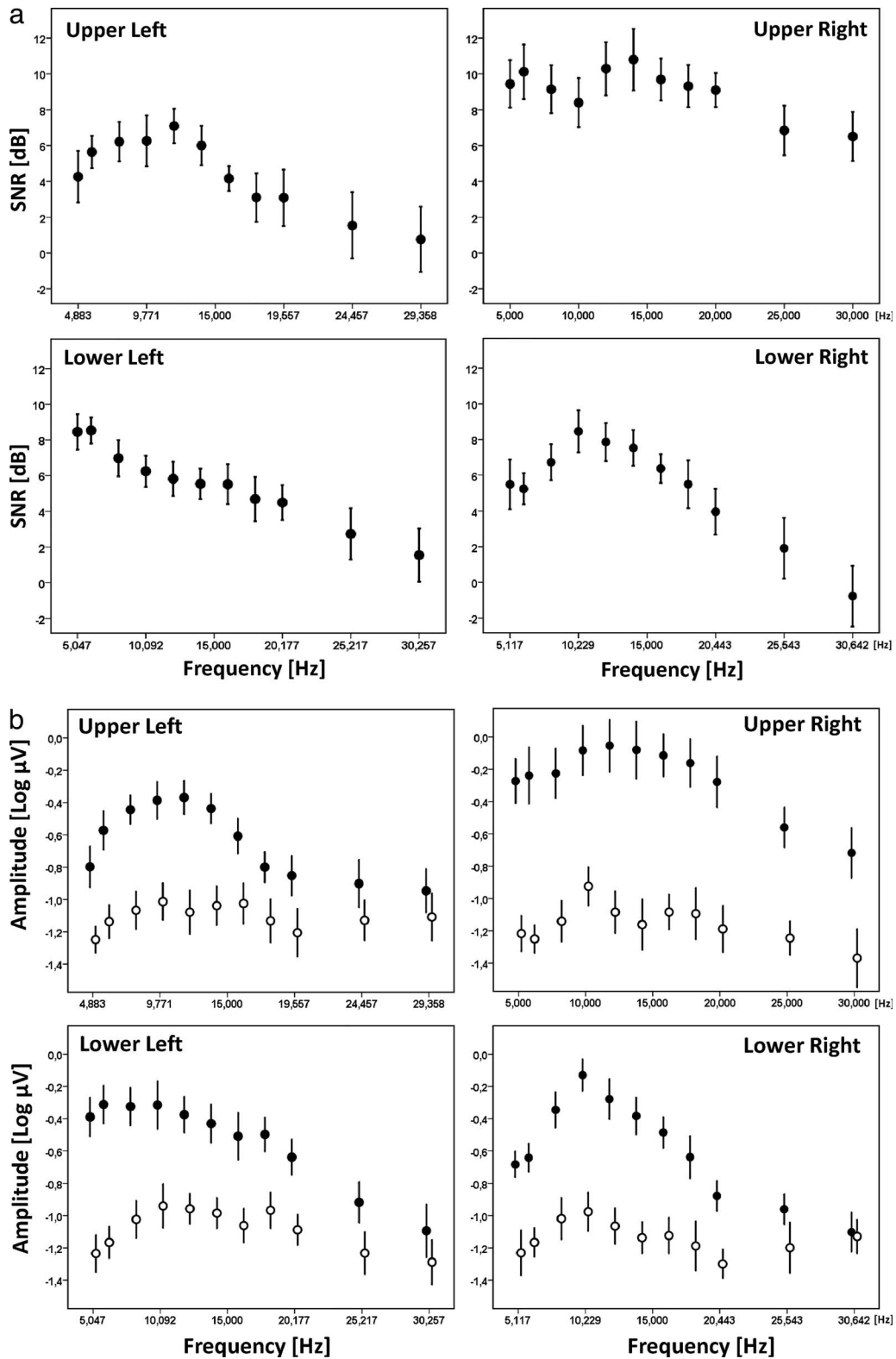


Figure 5. (a) SNR (± 95 CI) from 10 healthy subjects plotted as a function of temporal frequency (Hertz) for all four LED arrays. (b) *Filled symbols*: mean amplitudes (microvolts) (± 95 CI) from all subjects as a function of stimulus frequency plotted for different positions of the stimulation field. Maximal signals were recorded in the *upper-right* LED array. For all stimulus positions, a maximal amplitude was observed at 10 or 12 Hz. *Open symbols*: amplitudes calculated at two nonstimulus frequencies (noise level).

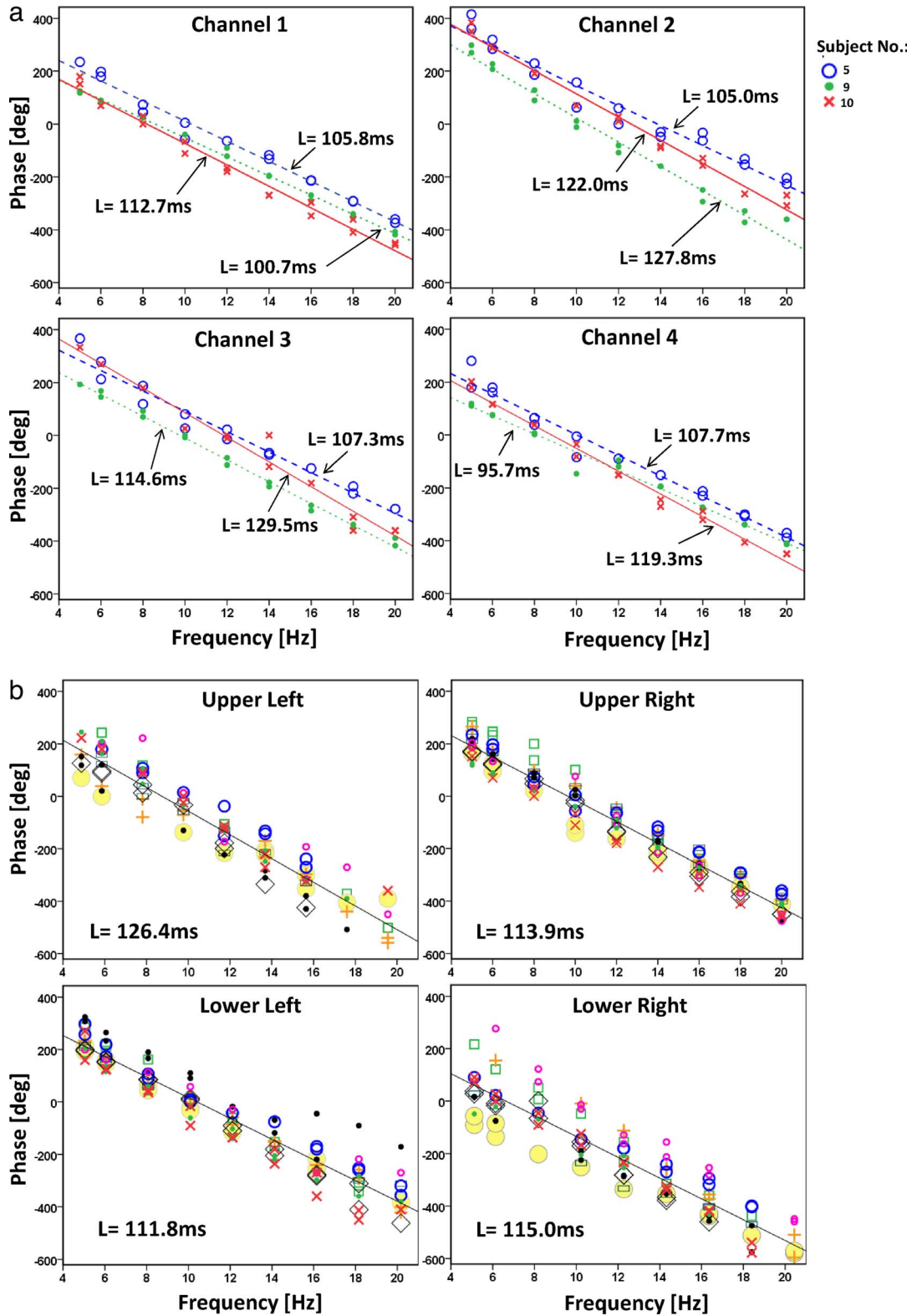


Figure 6. (a) Phase values from three subjects for different channels at one stimulus location (*upper right*). The figures show individual linear regression lines and indicate good reproducibility of the phase values from first and second measurement by *equal symbols*. Eleven percent (23/216) of the phase values were excluded because corresponding amplitudes were low at this stimulus position. An algorithmic latency value for each subject has been calculated by the slope of the regression line using the formula (in milliseconds):

→

←
latency = $-\left[(\Delta\text{phase}/\Delta F) \times 1000 \text{ ms}/360^\circ\right]$. (b) Phase values for all quadrants at channel 1 (i.e., electrodes above and below from inion). At this electrode position, the SNR values were larger than 2 dB in 75% (538/720) of the cases. The figures also show regression lines and indicate algorithmic latencies for the total cohort.

algorithmic latency is proportional to the slope of the phase versus frequency plot. For the measurements at the right upper quadrant, whose data are shown in Figure 6a for all channels, the individual algorithmic latencies varied between 95.7 and 129.5 ms. Figure 6b displays the phases and algorithmic latencies at channel 1 for four quadrants from all subjects. The mean of the slope (\pm SD) was upper left: -45.5 ± 6.2 deg/Hz; upper right: -41.0 ± 3.2 deg/Hz; lower left: -40.2 ± 3.6 deg/Hz; and lower right: -41.4 ± 6.8 deg/Hz. Thus, the mean algorithmic latency for the subjects was between 111.8 ± 10.0 and 126.4 ± 17.3 ms. The response phases elicited by the left upper quadrant had a slightly steeper slope compared to those evoked by the right upper and lower left quadrants (Wilcoxon test: $P = 0.05$). The intercept of the linear regression for the lower-right quadrant differed by approximately 180° in comparison to the others, indicating an inverted signal at this location.

Discussion

The aim of this study was to investigate the feasibility of obtaining reliable and well-separated VEPs from spatially separated stimuli in normal subjects using a four-channel recording system and simultaneous pattern-reversal stimulation using LED arrays. The stimulus frequency in the LED arrays differed slightly. This difference could be resolved in the analysis of the signals so that the responses elicited by the four LED arrays could be identified. The differences were, however, small enough to ensure that identical physiological mechanisms can be expected to mediate the responses. Earlier studies showed a potential usefulness of the multifrequency LED stimulation technique in the ERG.^{8,15–17} We show here that the responses from LED arrays, located at different positions in the visual field, can be reliably measured in the VEP. The use of LEDs has several advantages: they have excellent temporal properties and can be used to deliver temporal frequencies with high precision. In addition, LED fields can reach high luminances and contrasts and can be spatially homogeneous. Frequency differences, used in the present study, are difficult to achieve with monitors that have refresh rates of maximally 200 Hz.¹⁸ Furthermore, the pixels of monitors are

generally refreshed sequentially, thereby introducing stimulus delays that depend on the spatial position. Recently, a method to increase the frequency resolution on a conventional monitor was introduced by Nakanishi et al.¹⁹ using a variable number of frames in a period. However, in contrast to the present study they did not present several pattern-reversal targets simultaneously. So far, quadrant recordings with pattern-reversal stimulation were made with separate stimulation of each field quadrant.^{20–22} More recently, Maddess and colleagues²³ demonstrated the value of the incommensurate frequency technique for grating stimulation on a monitor with several discrete reversal frequencies. In the present study, we show that LEDs can be used in arrays that can deliver pattern-reversal stimuli with very small temporal frequency differences. Other studies used LED as well,^{8,24–28} although they were not yet implemented in clinical routine despite their advantages over monitors. Currently, LEDs are increasingly used in brain computer interface techniques for steady-state stimulus presentations.²⁹ The disadvantage of LED arrangements compared to monitor systems, where pattern with complex structure and distortion can be easily generated, is the lack of geometric flexibility. In our LED arrays, the spatial frequency can only be altered by changing the viewing distance. Here, we used a distance of 30 cm, resulting in a total stimulus field size of $20.8^\circ \times 20.8^\circ$ and a constant spatial frequency of 0.58 cyc/deg. Due to the relative large rim at the edge of each LED array, we were not able to measure the central quadrant VEP. On the other hand, larger LED arrays would be needed for more peripheral stimulation. Thus, development of LED arrays that consider the scaling of the VEP amplitudes to eccentricity could possibly improve the SNR values.

Recordings of signals derived from several focal stimuli can be performed sequentially,^{20,30} by a multifrequency method,⁸ or by the m-sequence technique as introduced by Sutter and Tran.⁹ Sutter showed that the responses to multiple simultaneously presented stimuli can be reconstructed by cross-correlation, resulting in a topographical VEP recording system. It has been shown that the m-sequence technique can be used for transient stimulation as well as for steady-state measurements⁴ using a conven-

tional monitor. In measurements by Horn et al.,⁴ only half of the stimulation fields was flickering at the same time, while the other half was not activated. In the present LED-array arrangement, all stimuli were presented simultaneously, consequently requiring less examination time as the m-sequence technique. The data were continuously acquired at a sufficiently high rate without averaging and subsequently spectrally analyzed to resolve the frequency differences between the outputs of the different LED arrays (see, e.g., Fig. 2). Please note that the present FFT technique used relative long registration periods for one single measurement that cannot be interrupted. This was done to demonstrate the high-frequency resolution of the visual system. However, in the midfrequency range, the recordings were sufficiently short for clinical application (e.g., 91.5 seconds at 12 Hz). This is close to the resolution presented earlier.^{5,31}

Beyond showing the feasibility of simultaneously stimulated quadrant VEP our aim was to study the influence of the stimulus frequency on the responses and to find the optimal stimulus frequency. For all four arrays, the stimulus frequency resulting in the maximal VEP response was between 10 and 12 Hz. This is in agreement with previous studies.^{4,32,33} Furthermore, the amplitudes were similar to those found previously in experiments using conventional multifocal stimuli³⁴ and with the steady-state multifocal VEP.⁴ However, in contrast to earlier studies where the amplitudes were largest in the lower stimulus fields,^{20,35,36} we found the largest amplitudes in the upper-right quadrant. Further studies are necessary to reveal whether this difference in results is a possible effect of differences in size and spatial arrangement of the stimuli. The SNR is a useful tool that can be helpful to judge the quality of the measurements and to determine which of the simultaneously derived VEP signals might be taken for further analyzes.^{4,37} In steady-state responses, the SNR can be calculated by dividing the amplitude at the stimulus frequency by the amplitudes at adjacent frequencies where no response to the stimulus is expected. The temporal resolution in the present study, results in at least nine nonstimulus frequencies between the stimulus frequencies (see Fig. 2). Here we always used the next but one adjacent reversal frequency for the SNR calculation because we sometimes observed some leakage of energy to directly neighboring frequencies. The shape of the tuning function was very similar for SNR and amplitudes. With this technique, the SNR values are larger than 2 dB for most tests between 6 and 20 Hz.

The SNR might be different if other or more nonstimulus frequencies were included.³⁸

Response phases were analyzed in the present study. Most previous multifocal VEP studies are restricted to amplitudes as cortical signals derived from the stimulation of different segments can show opposite polarities.³⁹ In addition, it is often not easy to allocate an absolute phase from a steady-state derivation because the FFT returns phases only in a range of 360°. In the present study (see example in Fig. 6a), an absolute phase is not measured either. Instead, a frequency-dependent phase change was obtained. The phase dependency on stimulus frequency was approximately linear for all LED arrays, with similar slopes indicating similar apparent latencies for all subjects and LED arrays of 111.8 to 126.4 ms. This is close to the peak latencies measured in conventional transient VEPs. Furthermore, our data are comparable to the latency values as found by Di Russo and Spinelli⁴⁰ in a steady-state study (122 ms). The algorithmic latency with localized stimulation may be different in patients with structural or functional damages (such as multiple sclerosis).^{41,42}

Conclusion

Multifrequency stimulation using quadrant LED arrays may be a promising and efficient method for recording of pattern-reversal VEPs. The optimal frequency was 12 Hz stimulus frequency, and apparent latencies varied between 112 and 126 ms.

Acknowledgments

The authors thank Edith Moncziaak for skillful technical assistance. The development of the present multifrequency technology was supported by the ELAN program of the Friedrich-Alexander-University Erlangen-Nürnberg. The authors have no commercial interest in the equipment used in this work.

Disclosure: **B. Hohberger**, None; **J. Kremers**, None; **F.K. Horn**, None

References

1. Regan D. Some characteristics of average steady-state and transient responses evoked by modu-

- lated light. *Electroencephalogr Clin Neurophysiol*. 1966;20:238–248.
2. Perlstein WM, Cole MA, Larson M, Kelly K, Seignourel P, Keil A. Steady-state visual evoked potentials reveal frontally-mediated working memory activity in humans. *Neurosci Lett*. 2003;342:191–195.
 3. Gray M, Kemp AH, Silberstein RB, Nathan PJ. Cortical neurophysiology of anticipatory anxiety: an investigation utilizing steady state probe topography (SSPT). *Neuroimage* 2003;20:975–986.
 4. Horn FK, Selle F, Hohberger B, Kremers J. Steady-state multifocal visual evoked potential (ssmfVEP) using dartboard stimulation as a possible tool for objective visual field assessment. *Graefes Arch Clin Exp Ophthalmol*. 2016;254:259–268.
 5. Kusel R, Wesemann W, Rassow B. A new laser interferometer for the stimulation of pattern-reversal visual evoked potentials. *Clin Phys Physiol Meas*. 1985;6:239–246.
 6. Regan MP, Regan D. Objective investigation of visual function using a nondestructive zoom-FFT technique for evoked potential analysis. *Can J Neurol Sci*. 1989;16:168–179.
 7. Cartwright RF, Semi-automatic, Regan D. multi-channel Fourier analyser for evoked potential analysis. *Electroencephalogr Clin Neurophysiol*. 1974;36:547–550.
 8. Lindenberg T, Horn FK, Korth M. Cyclic summation versus m-sequence technique in the multifocal ERG. *Graefes Arch Clin Exp Ophthalmol*. 2003;241:505–510.
 9. Sutter EE, Tran D. The field topography of ERG components in man—I. The photopic luminance response. *Vision Res*. 1992;32:433–446.
 10. Zhang X, Hood DC, Chen CS, Hong JE. A signal-to-noise analysis of multifocal VEP responses: an objective definition for poor records. *Doc Ophthalmol*. 2002;104:287–302.
 11. Link B, Ruhl S, Peters A, Junemann A, Horn FK. Pattern reversal ERG and VEP—comparison of stimulation by LED, monitor and a Maxwellian-view system. *Doc Ophthalmol*. 2006;112:1–11.
 12. Klistorner A, Graham SL. Objective perimetry in glaucoma. *Ophthalmology*. 2000;107:2283–2299.
 13. Hood DC, Zhang X, Hong JE, Chen CS. Quantifying the benefits of additional channels of multifocal VEP recording. *Doc Ophthalmol*. 2002;104:303–320.
 14. Meigen T, Bach M. On the statistical significance of electrophysiological steady-state responses. *Doc Ophthalmol*. 1999;98:207–232.
 15. Victor JD, Shapley RM, Knight BW. Nonlinear analysis of cat retinal ganglion cells in the frequency domain. *Proc Natl Acad Sci U S A*. 1977;74:3068–3072.
 16. Maddess T, James AC, Goldberg I, Wine S, Dobinson J. Comparing a parallel PERG, automated perimetry, and frequency-doubling thresholds. *Invest Ophthalmol Vis Sci*. 2000;41:3827–3832.
 17. Link B, Junemann A, Horn FK. Pattern reversal ERG with LED-stimulation using cyclic summation technique. *Doc Ophthalmol*. 2006;112:53–60.
 18. Abdullah SN, Vaegan, Boon MY, Maddess T. Contrast-response functions of the multifocal steady-state VEP (MSV). *Clin Neurophysiol*. 2012;123:1865–1871.
 19. Nakanishi M, Wang Y, Wang YT, Mitsukura Y, Jung TP. Generating visual flickers for eliciting robust steady-state visual evoked potentials at flexible frequencies using monitor refresh rate. *PLoS One*. 2014;9:e99235.
 20. Bradnam MS, Montgomery DM, Evans AL, et al. Objective detection of hemifield and quadrant field defects by visual evoked cortical potentials. *Br J Ophthalmol*. 1996;80:297–303.
 21. Horn F, Mardin C, Korth M, Martus P. Quadrant pattern ERG with SLO stimulation in normals and glaucoma patients. *Graefes Arch Clin Exp Ophthalmol*. 1996;234(suppl 1):S174–179.
 22. Cappin JM, Nissim S. Visual evoked responses in the assessment of field defects in glaucoma. *Arch Ophthalmol*. 1975;93:9–18.
 23. Abdullah SN, Aldahlawi N, Rosli Y, Vaegan, Boon MY, Maddess T. Effect of contrast, stimulus density, and viewing distance on multifocal steady-state visual evoked potentials (MSVs). *Invest Ophthalmol Vis Sci*. 2012;53:5527–5535.
 24. Evans BT, Binnie CD, Lloyd DS. A simple visual pattern stimulator. *Electroencephalogr Clin Neurophysiol*. 1974;37:403–406.
 25. Nilsson BY. Visual evoked responses in multiple sclerosis: comparison of two methods for pattern reversal. *J Neurol Neurosurg Psychiatry*. 1978;41:499–504.
 26. Epstein CM. True checkerboard pattern reversal with light-emitting diodes. *Electroencephalogr Clin Neurophysiol*. 1979;47:611–613.
 27. Czopf J. Flash and pattern presentation and pattern-reversal evoked potentials in multiple sclerosis. *Doc Ophthalmol*. 1985;59:129–141.
 28. Bueltmann S, Weimer P, Rohrschneider K. Flash visual evoked potentials in healthy volunteers and patients. *Invest Ophthalmol Vis Sci*. 2004;45:5486.

29. Zhu D, Bieger J, Garcia Molina G, Aarts RM. A survey of stimulation methods used in SSVEP-based BCIs. *Comput Intell Neurosci*. 2010;702357.
30. Horn FK, Korth M, Mardin C, Steinhauser B. Quadrant-pergs with stimulation by the Slo in normals and glaucoma. *Invest Ophthalmol Vis Sci*. 1995;36:S333.
31. Abdullah SN, Aldahlawi N, Rosli Y, Vaegan, Boon MY, Maddess T. Effect of contrast, stimulus density, and viewing distance on multifocal steady-state visual evoked potentials (MSVs). *Invest Ophthalmol Vis Sci*. 2012;53:5527–5535.
32. Heine M, Meigen T. The dependency of simultaneously recorded retinal and cortical potentials on temporal frequency. *Doc Ophthalmol*. 2004;108:1–8.
33. Maier J, Dagnelie G, Spekrijse H, van Dijk BW. Principal components analysis for source localization of VEPs in man. *Vision Res*. 1987;27:165–177.
34. Horn FK, Kaltwasser C, Junemann AG, Kremers J, Tornow RP. Objective perimetry using a four-channel multifocal VEP system: correlation with conventional perimetry and thickness of the retinal nerve fibre layer. *Br J Ophthalmol*. 2012;96:554–559.
35. Horn FK, Kaltwasser C, Junemann AG, Kremers J, Tornow RP. Objective perimetry using a four-channel multifocal VEP system: correlation with conventional perimetry and thickness of the retinal nerve fibre layer. *Br J Ophthalmol*. 2012;96:554–559.
36. Fortune B, Hood DC. Conventional pattern-reversal VEPs are not equivalent to summed multifocal VEPs. *Invest Ophthalmol Vis Sci*. 2003;44:1364–1375.
37. Meigen T, Bach M. On the statistical significance of electrophysiological steady-state responses. *Doc Ophthalmol*. 1999;98:207–232.
38. Vaegan, Rahman AMA, Sanderson GF. Glaucoma affects steady state VEP contrast thresholds before psychophysics. *Optom Vis Sci*. 2008;85:547–558.
39. Klistorner AI, Graham SL, Grigg JR, Billson FA. Multifocal topographic visual evoked potential: improving objective detection of local visual field defects. *Invest Ophthalmol Vis Sci*. 1998;39:937–950.
40. Di Russo F, Spinelli D. Effects of sustained, voluntary attention on amplitude and latency of steady-state visual evoked potential: a costs and benefits analysis. *Clin Neurophysiol*. 2002;113:1771–1777.
41. Falsini B, Porciatti V. The temporal frequency response function of pattern ERG and VEP: changes in optic neuritis. *Electroencephalogr Clin Neurophysiol*. 1996;100:428–435.
42. Lee J, Birtles D, Wattam-Bell J, Atkinson J, Braddick O. Latency measures of pattern-reversal VEP in adults and infants: different information from transient P1 response and steady-state phase. *Invest Ophthalmol Vis Sci*. 2012;53:1306–1314.